Applied Physics Reviews ARTICLE scitation.org/journal/are

A deep learning augmented genetic algorithm approach to polycrystalline 2D material fracture discovery and design

Cite as: Appl. Phys. Rev. 8, 041414 (2021); doi: 10.1063/5.0057162
Submitted: 18 May 2021 · Accepted: 24 November 2021 ·
Published Online: 10 December 2021

Andrew J. Lew[1,2] and Markus J. Buehler[1,3,a)]

AFFILIATIONS

[1]Laboratory for Atomistic and Molecular Mechanics (LAMM), Massachusetts Institute of Technology, 77 Massachusetts Ave., Cambridge, Massachusetts 02139, USA
[2]Department of Chemistry, Massachusetts Institute of Technology, 77 Massachusetts Ave., Cambridge, Massachusetts 02139, USA
[3]Center for Computational Science and Engineering, Schwarzman College of Computing, Massachusetts Institute of Technology, 77 Massachusetts Ave., Cambridge, Massachusetts 02139, USA

[a)]Author to whom correspondence should be addressed: mbuehler@mit.edu

ABSTRACT

The gestalt of computational methods including physics-based molecular dynamics simulations, data-driven machine learning (ML) models, and biologically-inspired genetic algorithms affords a powerful toolbox for tackling materials mechanism discovery and design problems. Here, we leverage these methods to investigate the complex multidimensional problem of polycrystalline 2D material fracture. We focus first on graphene and in doing so, demonstrate a practical workflow for exploring the structural dependencies of fracture energy. Despite training our ML model on exclusively single crystal fracture in increments of 10° orientations, we can identify a crack branching mechanism responsible for high bicrystal toughness centered at initial crystal orientation angles of 19° and 41°. These high peaks span only a few degrees in range and are completely overlooked by a search with stride 10°. Furthermore, we can discover qualitative physical phenomena such as collective fracture branch termination and extract quantitative trends relating angular dispersion and mis-orientation angles of crystal grains to fracture energy. None of these complex polycrystalline behaviors were presented in the training data, and the predictive power of the model ultimately allows us to expeditiously generate polycrystalline graphene structures with bespoke fracture paths, a task with great implications in industrial design applications and mechanism discovery. Furthermore, the approach is not limited to graphene specifically, as we demonstrate by retraining the model for another more complex 2D material—MoS_2—and achieve polycrystalline fracture predictions of comparable accuracy.

I. INTRODUCTION

Understanding, predicting, and ultimately controlling the fracture process is critically important to engineer materials. Molecular dynamics (MD) is a powerful tool that can precisely simulate fracture behavior at a detailed atomistic level. However, when considering the complexity of polycrystalline materials, the breadth of structural variables coupled with the computational cost of simulations makes it infeasible to gain a general understanding of fracture through MD alone, in spite of its bottom-up nature.

Though such a multidimensional problem is difficult to navigate, machine learning (ML) models are able to identify patterns and relationships within vast amounts of data for materials design[1,2] across various domains of data representation.[3] Classical computational materials science and ML methods can aid each other, by training ML models with simulation data and by replacing traditionally expensive calculations with ML methods.[4] The use of ML methods has accelerated the integration of materials science from discovery and design to extraction and application.[5]

Particularly, ML models in concert with finite element methods have assisted the design of composite materials[6] with optimized toughness.[7] Recent work in stress/strain field predictions[8] and elastic modulus identification[9] has honed in on modeling key mechanical material properties with deep learning. Furthermore, complex material design problems can be successfully tackled with inspiration from natural selection, through methods such as genetic algorithms[10] or the use of autoencoders to facilitate novel bio-inspired paradigms such as

converting fire to material designs.[11] In recent work, ML models have been used in tandem with genetic algorithms to design a diversity of material categories, from aluminum alloys[12] and dielectric polymers[13] to optical ceramics.[14] Deep learning models have seen recent success in the fracture prediction of simple Lennard-Jones models[15] and 2D materials such as single crystal graphene,[16] able to replicate trends from the training data and known graphene fracture behavior.

Here, we apply such an ML model in concert with a genetic algorithm metaheuristic[17] to the more complex fracture of polycrystalline 2D materials. In doing so, we identify previously unknown fracture mechanisms arising from the interplay of multiple crystal grains. Namely, particular bicrystal structure orientations that maximize fracture toughness and, in general, polycrystalline structures, probabilistic termination of branched fracture paths. It is often a concern that ML models have difficulty in extrapolating beyond the training data.[18] Importantly, the behaviors we identify are not indicated in any of the data used to train the ML model. Furthermore, the accuracy of model predictions facilitates targeted design of polycrystalline structures that fracture in precisely controllable ways. Our results can specifically be applied to the design of fracture resistant materials, but also serve as an example of how ML models can successfully extrapolate beyond their training conditions to discover new mechanisms of behavior that elucidate and gain insights into new physics.

II. RESULTS AND DISCUSSION

A. Fracture prediction methodology

Here, we first concern ourselves with structures of polycrystalline graphene. Specifically, we focus our discussion on rectangular geometries composed of i vertical strips with each grain's crystal lattice rotated to arbitrary orientations θ_i. For example, the bicrystal case is composed of two grains at orientations θ_1 and θ_2 as shown in Fig. 1(a).

This structural information is used as input into an ML model developed in detail in previous work[15,16] to predict fracture propagation. In short, the model shown in Fig. 1(b) incorporates convolutional layers to extract fracture features,[19] a long short-term memory (LSTM) unit[20] to extract the progressive relationship of propagation as a function of previous crack pattern, and a final dense layer to classify material locations as cracked or non-cracked.

Application of this ML model allows us to rapidly predict fracture behavior of various proposed graphene structures, such as the fracture paths shown in Fig. 1(c), without having to run a full MD simulation for each case. Instead, we only need single crystal MD data from select crystal orientations to train the ML model.

A priori, we expect that single crystal fracture may follow one of three broad directions: deflection upward, deflection downward, or horizontally straight. Accounting for branched paths taking two directions simultaneously (up and down, up and straight, or down and straight) gives us six broad categories of possible fracture types. Thus, to capture the space of potential fracture behaviors, we would desire at minimum six MD simulations per case. Using less than six MD simulations per case may miss out on crucial fracture branching behavior and may yield a biased ML model divorced from real fracture.

Conversely, using more than six MD simulations per case will allow us to gain a better understanding of the relative likelihoods of one fracture pattern type over another. Specifically, we use 11 MD fracture simulations each of single crystal graphene rotated in 10° increments, from 0° (zigzag) to 10°, 20°, and 30° (armchair) orientations, to provide a general representation of graphene fracture. This total of 44 images are shown overlaid per orientation in Fig. 1(d). Details of the simulation setup are described in Sec. IV.

B. Bicrystal fracture behavior

We first turn our attention to the simplest polycrystalline case for $i = 2$, bicrystal structures. Using the ML model for rapid fracture prediction, we map out bicrystal fracture energy as a function of the two crystal orientations, θ_1 and θ_2. We identify a greater dependence of

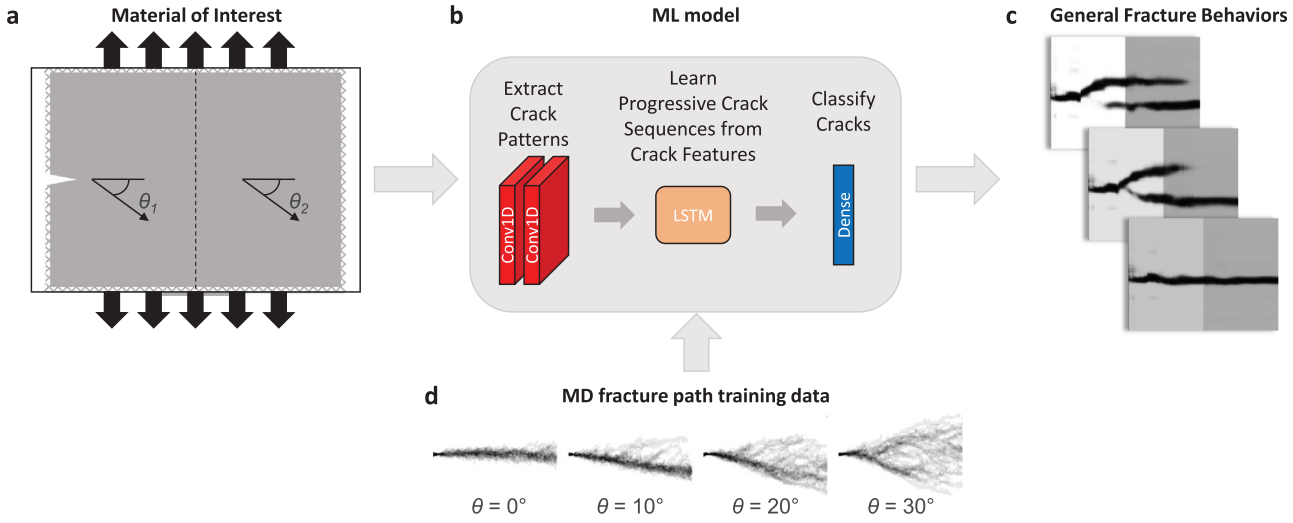

FIG. 1. In characterizing the mechanical properties of (a) polycrystalline graphene under Mode I tension with crystal orientations θ_i, (b) a machine learning classification model using an LSTM unit can be leveraged to (c) obtain fracture behavior of crystals with arbitrary orientations. With this machine learning method, (d) only a small set of simple single crystal molecular dynamics simulations are necessary to extrapolate general behavior of more complicated structures.

fracture energy on the orientation of the first crystal than the second, manifest as distinct bands in the energy surface along constant values for θ_1, as shown in Fig. 2(a).

Three features of θ_1 are observed—a broad peak centered about 30°, and two narrow satellite peaks at 19° and 41°. These peaks correspond qualitatively with increased fracture branching. Importantly, the fracture trends predicted by ML are corroborated by repeated MD simulations, which describe more crack branching at the peak orientations of 19°, 30°, and 41° than at other nearby orientations of 18°, 20°, 40°, and 42°, as shown in Fig. 2(b).

We hypothesize that these trends can be understood in terms of graphene's preference to fracture along the zigzag surface.[21] As the orientation increases toward 30°, the adjacent zigzag surface becomes available for fracture, resulting in the onset of crack branching as fracture can propagate toward both the upward and downward zigzag surfaces. This leads to the broad peak of fracture energy we see centered at 30°. However, a secondary effect centered around 30° occurs as well. At this point, the horizontal direction is directly in between zigzag surfaces and we see fracture paths have a chance of propagating straight[21] through to the second crystal. Fracture branching is reduced

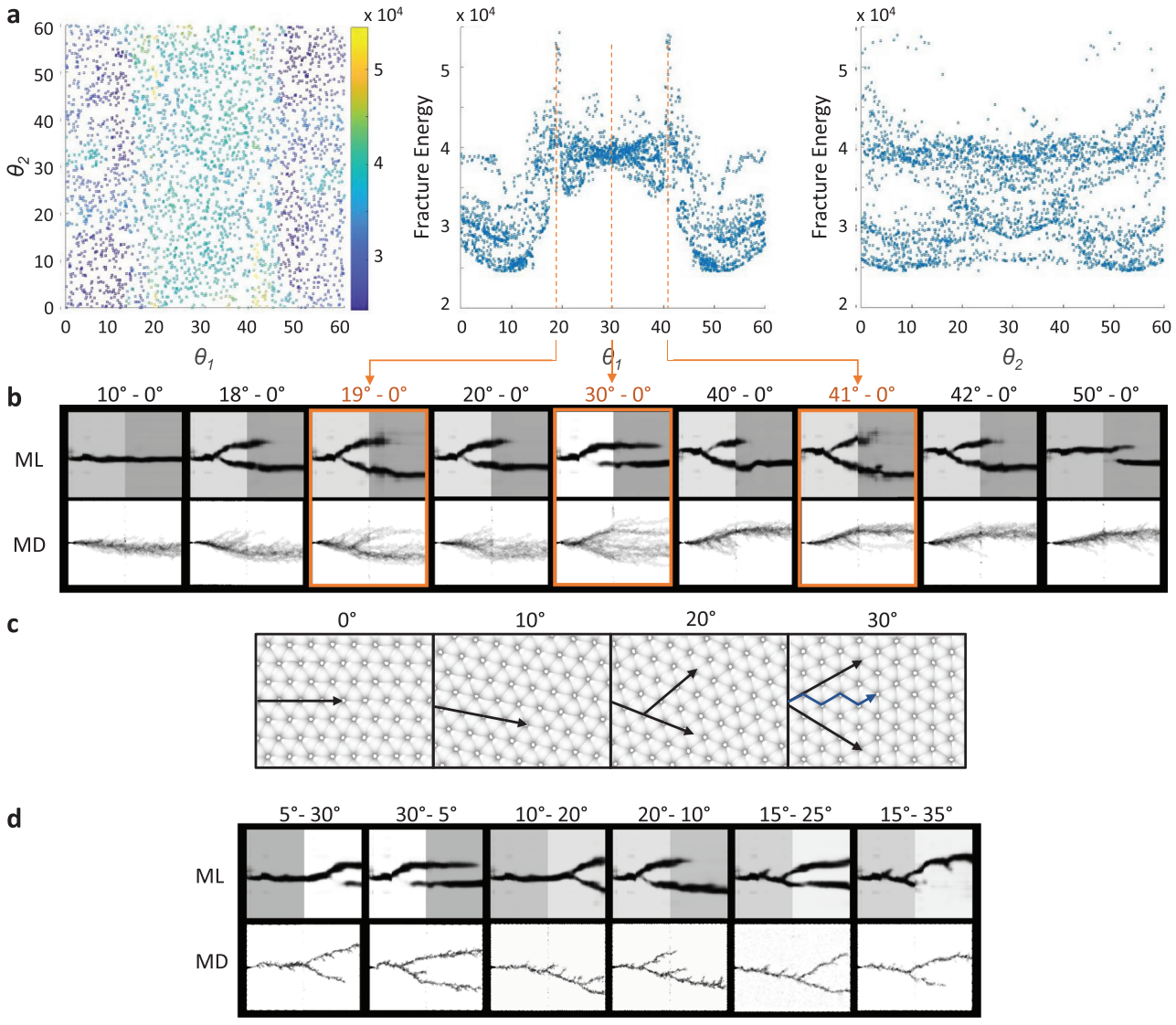

FIG. 2. The ML model can rapidly probe thousands of bicrystal orientations to (a) generate a fracture energy surface revealing distinct peaks and valleys. Fracture energy is more dependent on θ_1 than θ_2, with a broad band of increased energy centered about $\theta_1 = 30°$ accompanied by thin peaks along $\theta_1 = 19°$ and $\theta_1 = 41°$. Both the broad and fine trends are (b) corroborated by repeated MD simulations which show more fracture branching at the predicted peak values. This behavior can be understood by (c) considering the preference for graphene to fracture along zigzag surfaces, increasing fracture branching with increasing angle, overcome by a more direct fracture path available when rotated close enough to 30°. Despite being trained on only single crystal orientations, both these general trends and (d) specific predictions from the ML model closely agree with MD fracture paths.

when this occurs, leading to lower fracture energy[22] compared to the 19° or 41° cases. These fracture behaviors are visually illustrated in Fig. 2(c).

In addition to successfully identifying general fracture trends, specific MD simulations at various other selected angle combinations throughout the orientation space also align closely with the ML predictions, as in Fig. 2(d).

C. Polycrystalline fracture behavior

Even with the ML model expediting predictions, the design space of polycrystalline graphene fracture is vast. Fracture energy may be affected by the number of crystal grains, their orientations, and their sizes within the graphene sheet. To guide our search, we use a genetic algorithm outlined in Fig. 3(a) in concert with our ML model to generate graphene structures with desired fracture energies. Specifically, we define a fitness score to be the difference between a current structure's ML predicted fracture energy and a target value. Over multiple iterations of the genetic algorithm, we obtain structures closer to our target. Details of the genetic algorithm are provided in Sec. IV.

Running the genetic algorithm multiple times across a range of targets allows us to attain a series of polycrystalline graphene structures from low to high fracture energies. As can be seen in Fig. 3(b), we observe three distinct features in these ML predicted paths—straight line cracks, branched cracks, and vertical lines. Comparison to MD shows direct correspondence with the ML predicted straight and

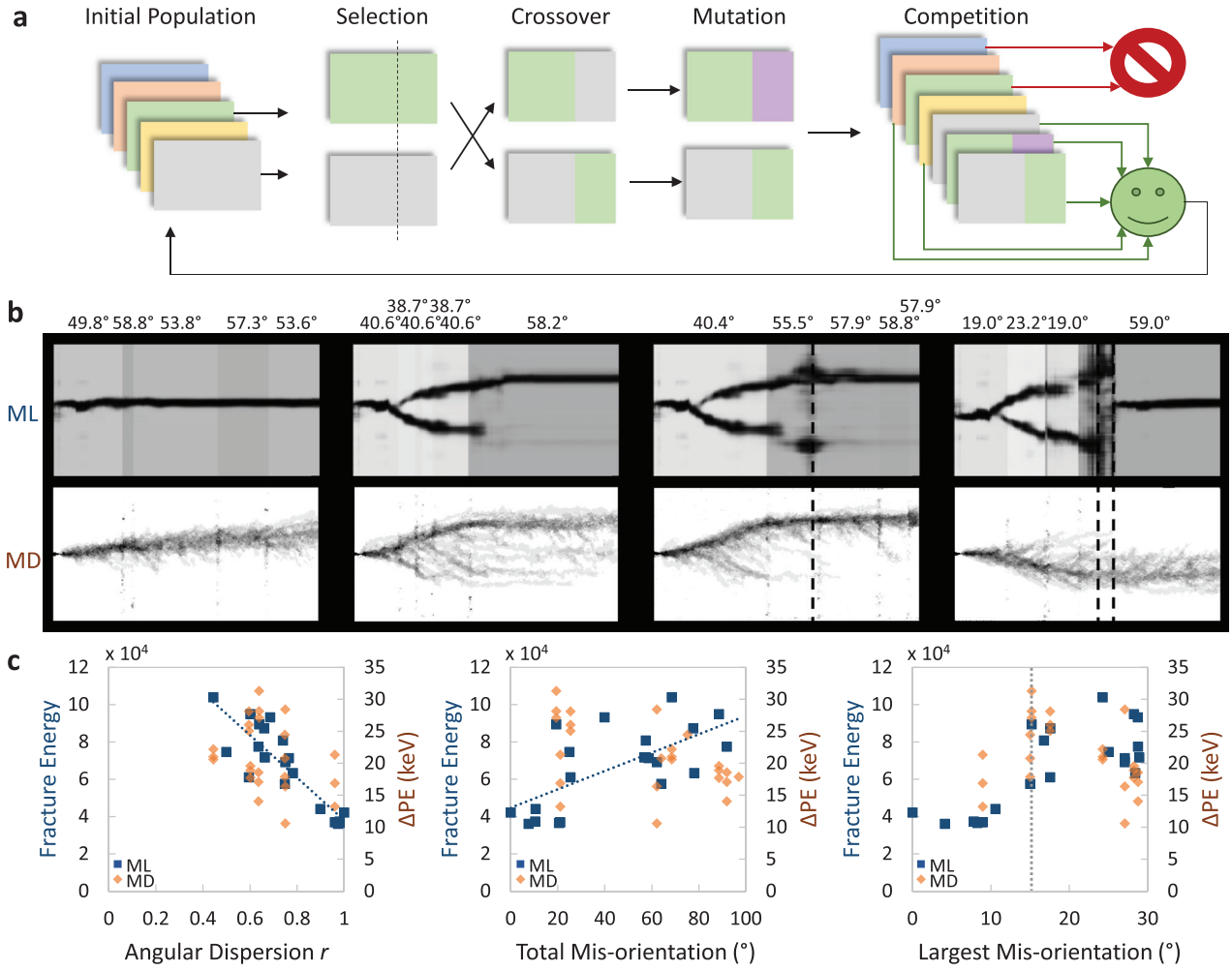

FIG. 3. The more general case of polycrystalline fracture with crystal grains of arbitrary number, orientation, and length can be explored using (a) a genetic algorithm to generate structures with targeted values of fracture energy. Across the range of accessible energies, (b) we see three distinct features in ML predicted fracture paths: straight cracks, branched cracks, and vertical lines. Predicted straight and branched cracks correspond directly to MD results, while vertical lines do not directly manifest in MD. Instead, these lines correspond to locations where crack branches tend to terminate. Quantitatively, we find (c) fracture energy correlates with structures with higher diversity in crystal orientations and with larger mis-orientations between grains. Specifically, fracture energies tend to increase when structures have mis-orientations above 15°—consistent with results from the bicrystal case.

branched cracks. However, the vertical line features are not representative of actual vertical cracks in the MD simulations. Instead, the positions of these vertical lines qualitatively correspond to the extent of crack branch penetration into the sample and locations of collective crack branch termination. In ML branched paths without clearly predicted vertical lines, the corresponding MD branches penetrate to various depths, with some extending fully to the other end of the sheet. In contrast, in cases where vertical lines are predicted by ML, we see more concerted behavior in the MD with a clear distinction before and after the line. Furthermore, the weight and clarity of the ML predicted vertical line correlate with the severity of the distinction in MD, with some cracks bleeding a short distance through the less distinct line in the third case of Fig. 3(b) compared to the much more distinct line predicted in the fourth case of Fig. 3(b).

Quantitatively, structure-property trends can be identified across the polycrystalline graphene samples. Structures with larger fracture energy tend to have more disperse crystal orientations, characterized by lower values of angular dispersion r, and larger mis-orientations between grains. Particularly, fracture energy increases when structures incorporate mis-orientation angles above 15°, consistent with the broad peak previously identified in the bicrystal case. These relationships are plotted in Fig. 3(c), and calculations for these quantities are detailed in Sec. IV.

D. Bespoke fracture design

The fitness metric directs the course of the genetic algorithm search. We can thus design for particular fracture paths by appending a spatially dependent term to the fitness. As shown in Fig. 4(a), we can define regions in space that alter the fitness of a proposed graphene structure. During the competition step of the genetic algorithm, we check how many pixels of predicted fracture paths intersect with the defined regions. To obtain fracture paths that avoid these regions, we can impose a fitness penalty proportional to the amount of intersection. Over the course of multiple generations of the genetic algorithm, we select for graphene structures not only with fracture behavior close to the target energy value but also with paths that avoid the penalty regions, as in Fig. 4(b). Importantly, running MD fracture simulations on these obtained graphene structures confirms that fracture paths indeed avoid the defined penalty regions, as shown in Fig. 4(c).

E. Generalization to MoS_2

MoS_2 is a hexagonal 2D material similar to graphene with a few key differences. Notably, it is composed of two elements instead of one, doubling the rotational angle of symmetry from 60° to 120°. Thus, in order to encapsulate the full range of fracture behaviors, we must similarly expand our training data from a 0°–30° range to a 0°–60° range. After retraining the ML model on 11 MD fracture simulations each of single crystal MoS_2 rotated at 0°, 10°, 30°, 50°, and 60° orientations, we obtain fracture predictions with good qualitative agreement with the fracture behavior detailed by MD simulations shown in Fig. 5(a).

Quantitatively, our model has a low loss of 0.08 and high accuracy of 0.98 after training for 200 epochs, with good agreement between training and validation sets. These results, shown in Fig. 5(b), inform us that the model has learned fracture propagation relationships without overfitting. Furthermore, the complexity of the predicted fracture patterns, measured in terms of the fractal dimension[23] in Fig. 5(c), agrees well with MD. ML predictions have only an average underestimation of 0.1 fractal dimension, the same level of discrepancy as our previous graphene results.[16] In terms of crack length, shown in Fig. 5(d), the ML predictions capture the general u-shaped trend as a function of orientation but tend to underestimate the frequency of crack branching at higher angles, resulting in a deviation to lower values than MD that subsequently affects the values of predicted crack

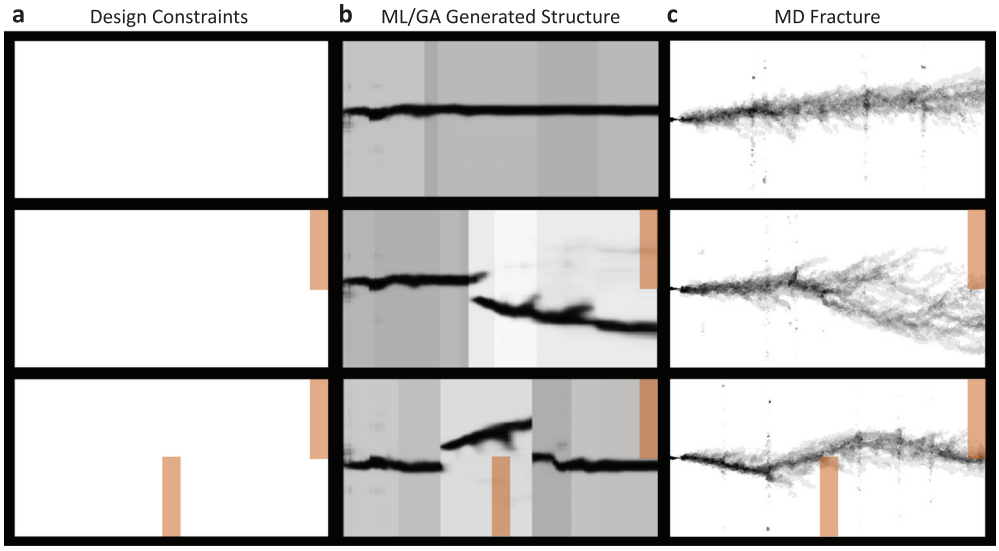

FIG. 4. Achieving a desired fracture behavior by introducing a penalty term to the fitness function that reduces structure fitness when predicted fracture crosses (a) defined regions we wish to avoid. By running the genetic algorithm with these penalties, we (b) generate proposed graphene structures that satisfy the input constraints. In this case, we have selected for the most direct paths which avoid penalty regions. (c) MD simulations confirm desired fracture behavior with paths that swerve away from these regions.

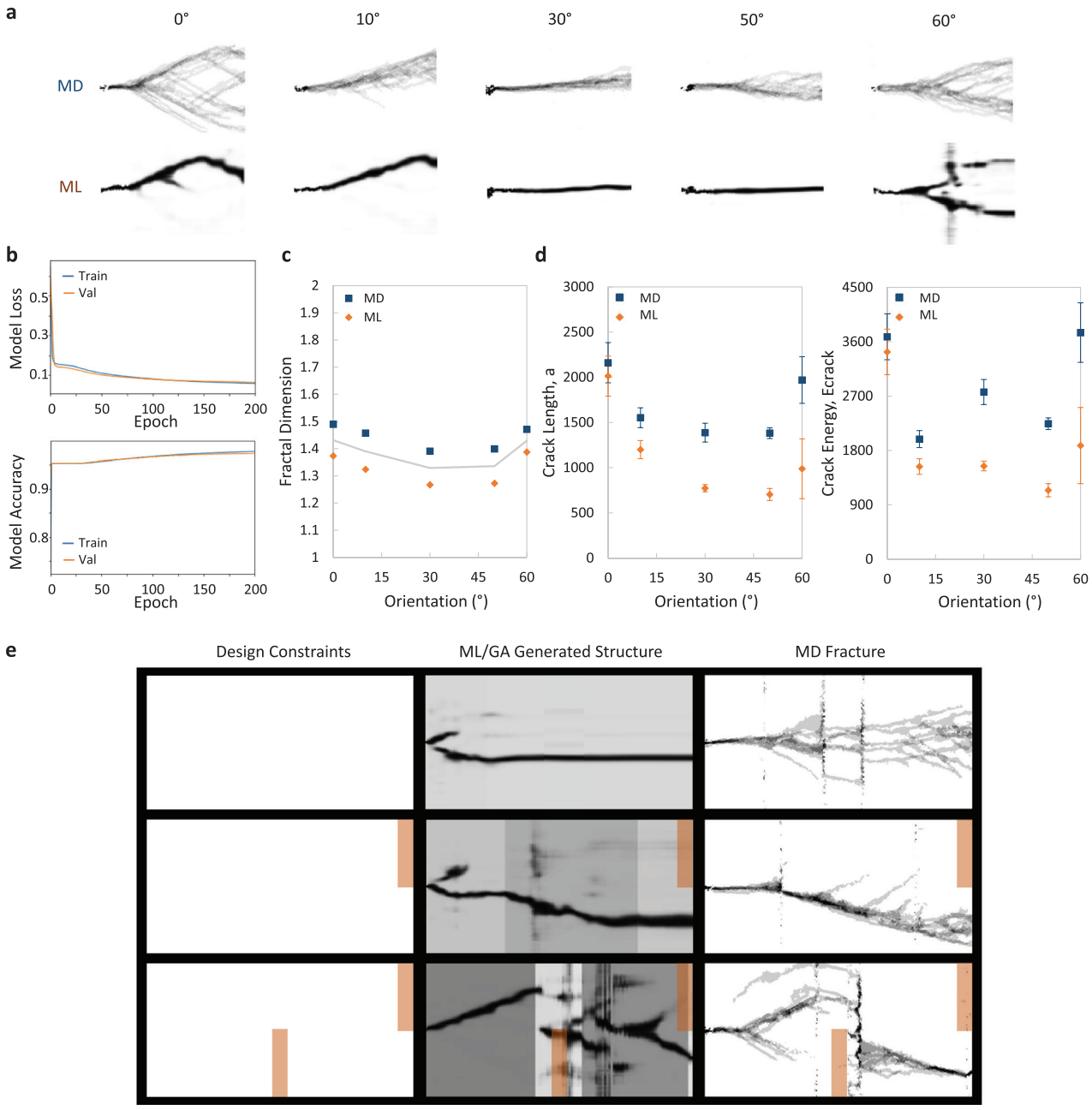

FIG. 5. Training the model on MoS_2 fracture paths yields (a), fracture predictions of similar quality as those for graphene with (b), model loss of 0.08 and model accuracy of 0.98. There is good quantitative agreement between the (c) fractal dimension of the MD and ML predicted fracture paths, with the same low level of discrepancy as present in previous graphene studies. (d) Predicted crack lengths and crack energies also follow a similar trend to the MD results, though tend to underestimate values at higher angles. Regardless, (e) the model can still be used to direct the design of complex polycrystalline structures that avoid fracture within certain prescribed areas, demonstrating the generalizability of our approach to multiple material systems.

energies at these angles. However, this underestimation does not impact the model's ability to successfully predict the fracture patterns of polycrystalline MoS_2 which, in concert with the spatially dependent genetic algorithm search, can still be used to design structures with desired fracture paths shown in Fig. 5(e).

III. CONCLUSION

MD simulations are powerful tools in modeling material fracture. However, in the task of probing general trends, fine behavior can be easily missed without conducting a prohibitively expensive degree-by-

degree orientation angle search. The efficiency of ML predictions allows us to more feasibly explore the graphene parameter space with enough fidelity to identify detailed behavior, such as the thin counter-intuitive fracture energy peaks of bicrystal graphene at $\theta_1 = 19°$ and $\theta_1 = 41°$. These peaks arise from a combination of competing factors affecting crack branching about $\theta_1 = 30°$ as described previously with Fig. 2(c). While the intermediary points maximizing fracture branching between 0°/60° and 30° could be probed with repeated MD, here our model quickly identifies the angles of interest as a 'magnet' pulling out our proverbial needle-in-the-haystack and thus enhances our ability to discover interesting behavior.

In the case of polycrystalline fracture, the parameter space is so large that one may not always have precognition of what behaviors to expect. In predicting fracture branch termination as with Fig. 3(b), the ML model helps us target structures of interest for more expensive MD simulation. Discovering this behavior *a priori* would require blind simulation of a vast variety of structures in the hope something interesting would be found. Furthermore, such a search would have to be conducted multiple times over, as the fracture termination behavior is a statistical one that only becomes apparent over an ensemble of fracture paths. In this sense, our model can also act as a "searchlight" into the unknown, assisting the discovery of mechanisms we may not have known were there and are easy to miss otherwise.

Directing our simulations with genetic algorithm search techniques affords us a powerful workflow able to investigate particular spaces of interest and even design structures to specific criteria. While there is nothing theoretically preventing MD-based searches, to explore the fracture of 3000 structures at a rate of 2 h per simulation would take in total 250 days of constant simulation time, using 6 Centos7 nodes with 96 CPUs and 1 GPU on the high performance MIT Engaging compute cluster. Comparatively, the fracture of those 3000 structures can be predicted with our ML model in a total of only 10 h on a local laptop with an Intel® Core™ i7–10750H Processor. This drastic reduction in computational resources, and time by 99.8%, brings such theoretical design workflows into practical use. Though the problem of fracture is incredibly complex, we can successfully predict fracture in both qualitative and quantitative terms and controllably attain structures that fracture in just the way we desire. Our example in designing materials with specifically deflected fracture paths as in Fig. 4 may be of particular use in the design of electronics or components where it is critical to avoid failure in certain regions.[24]

This combination of genetic algorithm-directed searches of ML surrogate models trained on MD fracture data is directly generalizable to material systems other than graphene. MoS_2 is a more complicated 2D material in terms of chemical composition, layered geometry, and symmetry. But despite these added complexities, the approach yields qualitative and quantitative predictions for MoS_2 comparable to the graphene case as in Fig. 5. So long as an appropriate training dataset exists or can be obtained, our approach is material system agnostic and may be used for both fundamental investigations into material behavior and applied design problems.

Further work remains in generalizing the considered fracture conditions. Cases of interest may include additional loading beyond Mode I fracture and structures including crystal grains of non-rectangular shape. Furthermore, the ability to treat materials of dimensionality beyond 2D sheets would bring us another step closer toward a general design tool for materials failure, especially if it could be combined with automatic material processing and testing[25,26] in an experimental environment. While there is more work to be done before reaching that point, the application of ML methods to materials fracture can not only interpolate between training points to match known trends as in previous work, but also extrapolate to the discovery of new mechanisms previously beyond our reach.

IV. METHODS

A. Molecular dynamics (MD) simulations

All graphene molecular dynamics simulations are performed using LAMMPS[27] and the reactive AIREBO[28] potential. Though there are noted discrepancies in AIREBO energy predictions of armchair and zigzag edges compared to *ab initio* calculations,[29] this potential can well characterize carbon allotropes[30,31] and has often been used to model elastic mechanics of graphene[32,33] in the literature. MoS_2 simulations are also performed using LAMMPS, but use the REBO-MoS_2 potential found in the literature[34,35] with optimized parameters from more recent density functional theory (DFT) studies.[36] Samples are equilibrated with a Nosé–Hoover thermostat[37] at a constant temperature of 300 K and barostat with a constant pressure of 0 bar in the tensile direction for 50 ps.

Fracture is conducted at a strain rate of 0.0001% fs^{-1} with a time step of 1 fs. Periodic boundary conditions are applied in the tensile direction and non-periodic boundary conditions applied in the fracture and depth directions. During tensile tests, a 3 Å thick border is restricted to only allow motion in the tensile direction. As each fracture event is heavily affected by random molecular vibrations, multiple MD fracture simulations are run in order to illustrate a representative likely fracture behavior. The average fracture path is generated by overlaying individual fracture paths, summing the black intensity at each pixel location, and dividing by the number of image paths considered. The darker a pixel in the averaged image, the more frequently fracture paths went through that location for simulations of that structure.

B. Genetic algorithm for generating polycrystalline structures

The graphene and MoS_2 structures studied here are rectangular in shape, comprised themselves of rectangular crystal grains stretching uniformly across the tensile direction. As such, their structure can be represented by a code describing the crystalline orientation at each location along the length of the sheet. In this way, each two-dimensional polycrystalline sheet can be converted into a one-dimensional string of floats to act as a "gene" in our optimization algorithm. This method of encoding avoids convergence problems associated with large Hamming distances between certain adjacent values as present in traditional binary encoding methods.[38]

We start from an initial population of five bicrystal sheets with randomized crystal orientations and interface location. From this initial population, two sheets are randomly selected as parents for crossover, upon which a random index is selected as the crossover point. At this crossover point, the gene codes of the two selected sheets are cut and exchanged, forming two new genes describing two new structures. From here, we have implemented a variety of mutations that may occur to these offspring structures. First, the orientation of a crystal grain has a 30% chance of changing to a random angle. Second, two

crystal grains within a sheet have a 30% chance of swapping their orientations. Third, two adjacent crystal grains have a 10% chance of melding into one grain with an averaged orientation value. After the offspring have had a chance to mutate, they are compared with the original population with fracture energies predicted by the ML model. An energy dependent fitness score is assigned to each structure proportional to the distance from a target fracture energy value. A spatially dependent fitness term can be appended to select for particular fracture morphologies, by providing a fitness penalty to fracture paths that intersect forbidden spatial regions. The two least fit structures farthest away from the target value are discarded in a round of competition.

This new set of five polycrystalline sheets serves as the initial population for a next iteration of the algorithm, repeating the steps to generate structures ever closer to the target value. Here, we ran the algorithm for 100 iterations for each of the 20 structures generated for Fig. 3, targeting fracture energy values from 20 000 to 120 000. Despite this range of targets, only structures with fracture energy from about 40 000 to 100 000 were obtained, indicating that these may be the maximum and minimum values attainable for our rectangular polycrystalline graphene structures.

C. Energy trend calculations

Fracture energy of ML predicted fracture paths is calculated according to Eq. (1)

$$E_{crack} = \sum_i 2\gamma_i a_i B, \tag{1}$$

for a graphene sheet with crystal grains i, crack lengths a_i, and $B = 1$ for 2D materials. γ_i is calculated using Griffith's criterion[39] in Eq. (2)

$$\gamma_i = \frac{\pi {\sigma_{\max i}}^2 a_0}{2E_i}, \tag{2}$$

where σ_{max} and E for select crystal orientations are obtained from the stress-strain curves of single crystal MD simulations and a_0 is the length of the initial notch. For crystal orientations in between the single crystal MD training data orientations, γ is estimated by fitting a periodic sine function to the calculated points. Values for fracture energy calculated in this way are dependent on the crack lengths a, which are taken as the number of pixels classified as cracked by the ML model. As a result, energies are given in units proportional to keV by a pixel resolution-based constant. Fracture energy of MD simulated fracture paths can be directly estimated simply as the change in potential energy over the course of fracture.

The angular dispersion r is a metric for the monodispersity of a set of angular measurements, with 1 corresponding to a completely monodisperse ensemble and 0 corresponding to a uniformly distributed ensemble.[40] Specifically, this is calculated by Eq. (3),

$$r = \sqrt{\left(\frac{\sum_{i=1}^{n} \sin\theta_i}{n}\right)^2 + \left(\frac{\sum_{i=1}^{n} \cos\theta_i}{n}\right)^2}, \tag{3}$$

for number of angles n and angle values θ_i.

The total mis-orientation and largest mis-orientation angles are self-explanatory, taken simply as the sum of mis-orientation angles and the maximum value of mis-orientation angles within a graphene sheet, respectively.

D. Fractal dimension and crack length

As in previous work,[16] the Hausdorff fractal dimension of MD simulated and ML predicted fracture paths are calculated according to the traditional "box counting" method.[41] Specifically, we utilize a MATLAB tool implementing this "box counting" method[42] to calculate the fractal dimension from the monochrome fracture path images, where white corresponds to pristine structure and black corresponds to fracture. Accordingly, the crack lengths of each image are obtained by summing the number of black pixels and are provided in a unitless value proportional to nm by an pixel resolution-based constant. The values provided in Fig. 5(d) are over a sample size of N = 10 for each data point, with the error bars representing one standard deviation from the mean.

ACKNOWLEDGMENTS

This material is based upon work supported by the NSF GRFP under Grant No. 1122374. We acknowledge support by the Office of Naval Research (N000141612333 and N000141912375), AFOSR-MURI (FA9550-15-1-0514) and the Army Research Office (W911NF1920098). Related support from the IBM-MIT AI lab, MIT Quest, and Google Cloud Computing, is acknowledged.

AUTHOR DECLARATIONS

Conflict of Interest

The authors declare no conflict of interest.

Author Contributions

M.J.B. conceived the idea together with A.J.L. A.J.L. carried out the molecular dynamics simulations, machine learning predictions, implementation of the genetic algorithm, and subsequent analyses. M.J.B. supervised the project. A.J.L. wrote the manuscript with M.J.B.

DATA AVAILABILITY

The data that support the findings of this study are available from the corresponding author upon reasonable request.

REFERENCES

[1]K. Guo, Z. Yang, C.-H. Yu, and M. J. Buehler, "Artificial intelligence and machine learning in design of mechanical materials," Mater. Horiz. **8**, 1153–1172 (2021).
[2]R. Pollice *et al.*, "Data-driven strategies for accelerated materials design," Acc. Chem. Res. **54**, 849–860 (2021).
[3]M. J. Buehler, "Liquified protein vibrations, classification and cross-paradigm de novo image generation using deep neural networks," Nano Futures **4**, 35004 (2020).
[4]K. G. Reyes and B. Maruyama, "The machine learning revolution in materials?," MRS Bull. **44**, 530–537 (2019).
[5]S. Cranford, "Material lessons in machine learning," Matter **4**, 1431–1433 (2021).
[6]G. X. Gu, C. T. Chen, and M. J. Buehler, "De novo composite design based on machine learning algorithm," Extrem. Mech. Lett. **18**, 19–28 (2018).
[7]G. X. Gu, C.-T. Chen, D. J. Richmond, and M. J. Buehler, "Bioinspired hierarchical composite design using machine learning: Simulation, additive manufacturing, and experiment," Mater. Horiz. **5**, 939–945 (2018).

[8]Z. Yang, C.-H. Yu, and M. J. Buehler, "Deep learning model to predict complex stress and strain fields in hierarchical composites," Sci. Adv. **7**, eabd7416 (2021).
[9]B. Ni and H. Gao, "A deep learning approach to the inverse problem of modulus identification in elasticity," MRS Bull. **46**, 19–25 (2021).
[10]N. Chakraborti, "Genetic algorithms in materials design and processing," Int. Mater. Rev. **49**, 246–260 (2013).
[11]M. Milazzo and M. J. Buehler, "Designing and fabricating materials from fire using sonification and deep learning," iScience **24**, 102873 (2021).
[12]A. Praveen Sekhar, S. Nandy, S. Dey, S. Datta, and D. Das, "Multi-objective genetic algorithm based optimization of age hardening for AA6063 alloy," IOP Conf. Ser.: Mater. Sci. Eng. **912**, 052019 (2020).
[13]C. Kim, R. Batra, L. Chen, H. Tran, and R. Ramprasad, "Polymer design using genetic algorithm and machine learning," Comput. Mater. Sci. **186**, 110067 (2021).
[14]D. R. Cassar, G. G. Dos Santos, and E. D. Zanotto, "Designing optical glasses by machine learning coupled with a genetic algorithm," Ceram. Int. **47**, 10555–10564 (2021).
[15]Y. C. Hsu, C. H. Yu, and M. J. Buehler, "Using deep learning to predict fracture patterns in crystalline solids," Matter **3**, 197–211 (2020).
[16]A. J. Lew, C.-H. Yu, Y.-C. Hsu, and M. J. Buehler, "Deep learning model to predict fracture mechanisms of graphene," npj 2D Mater. Appl. **5**, 48 (2021).
[17]A. Hassanat *et al.*, "Choosing mutation and crossover ratios for genetic algorithms-a review with a new dynamic approach," Inf. **10**, 390 (2019).
[18]S. K. Kauwe, J. Graser, R. Murdock, and T. D. Sparks, "Can machine learning find extraordinary materials?," Comput. Mater. Sci. **174**, 109498 (2020).
[19]Y. LeCun, Y. Bengio, and G. Hinton, "Deep learning," Nature **521**, 436–444 (2015).
[20]S. Hochreiter and J. Schmidhuber, "Long short-term memory," Neural Comput. **9**, 1735–1780 (1997).
[21]Y. Chu, T. Ragab, and C. Basaran, "The size effect in mechanical properties of finite-sized graphene nanoribbon," Comput. Mater. Sci. **81**, 269–274 (2014).
[22]E. Smith, "The effect of crack front irregularity on the fracture toughness of brittle materials," Arch. Mech. **38**, 185–190 (1986).
[23]B. B. Mandelbrot, *The Fractal Geometry of Nature* (W. H. Freeman, 1983).
[24]Z. Gao, D. Li, G. Dong, and Y. F. Zhao, "Crack path-engineered 2D octet-truss lattice with bio-inspired crack deflection," Addit. Manuf. **36**, 101539 (2020).
[25]R. D. King *et al.*, "The automation of science," Science **324**, 85–89 (2009).
[26]K. Williams *et al.*, "Cheaper faster drug development validated by the repositioning of drugs against neglected tropical diseases," J. R. Soc. Interface **12**, 20141289 (2015).
[27]S. Plimpton, "Fast parallel algorithms for short-range molecular dynamics," J. Comput. Phys. **117**, 1–19 (1995).
[28]S. J. Stuart, A. B. Tutein, and J. A. Harrison, "A reactive potential for hydrocarbons with intermolecular interactions," J. Chem. Phys. **112**, 6472–6486 (2000).
[29]Y. Liu, A. Dobrinsky, and B. I. Yakobson, "Graphene edge from armchair to zigzag: The origins of nanotube chirality?," Phys. Rev. Lett. **105**, 235502 (2010).
[30]Z. Xu and M. J. Buehler, "Nanoengineering heat transfer performance at carbon nanotube interfaces," ACS Nano **3**, 2767–2775 (2009).
[31]J. H. Los, N. Pineau, G. Chevrot, G. Vignoles, and J. M. Leyssale, "Formation of multiwall fullerenes from nanodiamonds studied by atomistic simulations," Phys. Rev. B—Condens. Matter Mater. Phys. **80**, 155420 (2009).
[32]H. Zhao, K. Min, and N. R. Aluru, "Size and chirality dependent elastic properties of graphene nanoribbons under uniaxial tension," Nano Lett. **9**, 3012–3015 (2009).
[33]Q. X. Pei, Y. W. Zhang, and V. B. Shenoy, "A molecular dynamics study of the mechanical properties of hydrogen functionalized graphene," Carbon **48**, 898–904 (2010).
[34]T. Liang, S. R. Phillpot, and S. B. Sinnott, "Parametrization of a reactive many-body potential for Mo-S systems," Phys. Rev. B—Condens. Matter Mater. Phys. **79**, 245110 (2009).
[35]J. A. Stewart and D. E. Spearot, "Atomistic simulations of nanoindentation on the basal plane of crystalline molybdenum disulfide (MoS2)," Model. Simul. Mater. Sci. Eng. **21**, 045003 (2013).
[36]G. S. Jung *et al.*, "Interlocking friction governs the mechanical fracture of bilayer MoS2," ACS Nano **12**, 3600–3608 (2018).
[37]S. Nosé, "A molecular dynamics method for simulations in the canonical ensemble," Mol. Phys. **52**, 255–268 (1984).
[38]R. L. Haupt and S. E. Haupt, *Practical Genetic Algorithms* (John Wiley & Sons, Inc, 2004).
[39]A. A. Griffith, "VI. The phenomena of rupture and flow in solids," Philos. Trans. R. Soc. London. Ser. A, Containing Pap. Math. Phys. Charact. **221**, 163–198 (1921).
[40]S. R. Jammalamadaka and A. SenGupta, *Topics in Circular Statistics* (World Scientific, 2001).
[41]K. J. Falconer, "The Hausdorff dimension of self-affine fractals," Math. Proc. Cambridge Philos. Soc **103**, 339–350 (1988).
[42]A. Costa, see http://mathworks.com/matlabcentral/fileexchange/30329-hausdorff-box-counting-fractal-dimension for "Hausdorff (Box-Counting) Fractal Dimension" (MATLAB Central File Exchange, 2013).